Nature Medicine 13(11): 1333-1340, 2007

Tumor-induced anorexia and weight loss are mediated by the TGF-β superfamily cytokine MIC-1

Heiko Johnen[1,6], Shu Lin[2,6], Tamara Kuffner[1,6], David A Brown[1], Vicky Wang-Wei Tsai[1], Asne R Bauskin[1], Liyun Wu[1], Greg Pankhurst[1], Lele Jiang[1], Simon Junankar[1], Mark Hunter[1], W Douglas Fairlie[1], Nicola J Lee[2], Ronaldo F Enriquez[2], Paul A Baldock[2], Eva Corey[3], Fred S Apple[4], MaryAnn M Murakami[4], En-Ju Lin[5], Chuansong Wang[5], Matthew J During[5], Amanda Sainsbury[2], Herbert Herzog[2,6] & Samuel N Breit[1,6]

[1]Centre for Immunology, St. Vincent's Hospital and University of New South Wales, and [2]Neuroscience Program, Garvan Institute of Medical Research, Sydney, New South Wales 2010, Australia. [3]Department of Urology, University of Washington, Seattle, Washington 98195, USA. [4]Clinical Laboratories, Hennepin County Medical Center, and University of Minnesota School of Medicine, Minneapolis, Minnesota 55415, USA. [5]Human Cancer Genetics Program, The Ohio State University, Columbus, Ohio 43210, USA. [6]These authors contributed equally to this work.

Anorexia and weight loss are part of the wasting syndrome of late-stage cancer, are a major cause of morbidity and mortality in cancer, and are thought to be cytokine mediated. Macrophage inhibitory cytokine-1 (MIC-1) is produced by many cancers. Examination of sera from individuals with advanced prostate cancer showed a direct relationship between MIC-1 abundance and cancer-associated weight loss. In mice with xenografted prostate tumors, elevated MIC-1 levels were also associated with marked weight, fat and lean tissue loss that was mediated by decreased food intake and was reversed by administration of antibody to MIC-1. Additionally, normal mice given systemic MIC-1 and transgenic mice overexpressing MIC-1 showed hypophagia and reduced body weight. MIC-1 mediates its effects by central mechanisms that implicate the hypothalamic transforming growth factor-β receptor II, extracellular signal–regulated kinases 1 and 2, signal transducer and activator of transcription-3, neuropeptide Y and pro-opiomelanocortin. Thus, MIC-1 is a newly defined central regulator of appetite and a potential target for the treatment of both cancer anorexia and weight loss, as well as of obesity.

Weight and appetite control are complex, incompletely characterized processes whose dysregulation can lead to obesity or anorexia. In late-stage cancer, it is believed that tumor- or stromal cell–derived molecules disturb the stringent control of appetite and weight control, leading to wasting, debility and often death[1, 2, 3, 4, 5, 6]. Interleukin-6 (IL-6) has been considered the likeliest etiological agent of anorexia and cachexia, although several cytokines have been implicated in this process.

MIC-1, also called GDF-15, PLAB, PDF or NAG-1, is a transforming growth factor-β (TGF-β) superfamily protein. It is not expressed under basal conditions but may be induced by inflammation, injury or malignancy[7, 8, 9, 10, 11, 12, 13]. MIC-1 is overexpressed in many cancers, including those of the prostate, colon, pancreas and breast[14]. In individuals with advanced cancer, serum MIC-1 can rise from a mean of 0.45 ng/ml to 5–50 ng/ml or higher. Individual tumors vary in the amount of MIC-1 they secrete because of differences in expression level and variation in the processing of mature MIC-1 by pro-convertases[11].

Here we examine the consequences of elevated circulating levels of MIC-1 and show that tumors overexpressing MIC-1 induce anorexia, which can be reversed by administration of antibodies to MIC-1 and mimicked by injection of recombinant MIC-1. We further show a direct correlation between serum MIC-1 levels and weight loss in individuals with advanced prostate cancer or chronic renal failure. In addition, we show that MIC-1 modulates neuronal pathways important in the regulation of appetite and energy homeostasis.

RESULTS

MIC-1 induces rapid weight loss reversed by antibodies to MIC-1

To understand the effects of systemic overexpression of MIC-1, we stably transfected the human prostate cancer cell line DU145 with human MIC-1 (MIC-1) constructs and injected these cells subcutaneously (s.c.) into the flanks of nude mice to establish xenografted tumors[11]. Mice were weighed regularly and killed after 6 weeks. Those with elevated amounts of tumor-derived human MIC-1 progressively lost weight (Figs. 1 and 2a,b). Mice with low serum levels of tumor-derived human MIC-1 (0–1,500 pg/ml), similar to levels found in normal humans, gained about 19% body weight, consistent with the young age of these mice (Fig. 1a). Mice with moderately elevated MIC-1 (1,501–8,500 pg/ml) lost 3% of body weight, and those with markedly elevated MIC-1 (>8,500 pg/ml) lost 28% of body weight (Fig. 1a). As mice with control tumors continued to gain weight, the net relative effect of MIC-1 was a 22% and 47% reduction in weight of mice with moderate and high serum levels of human MIC-1, respectively.

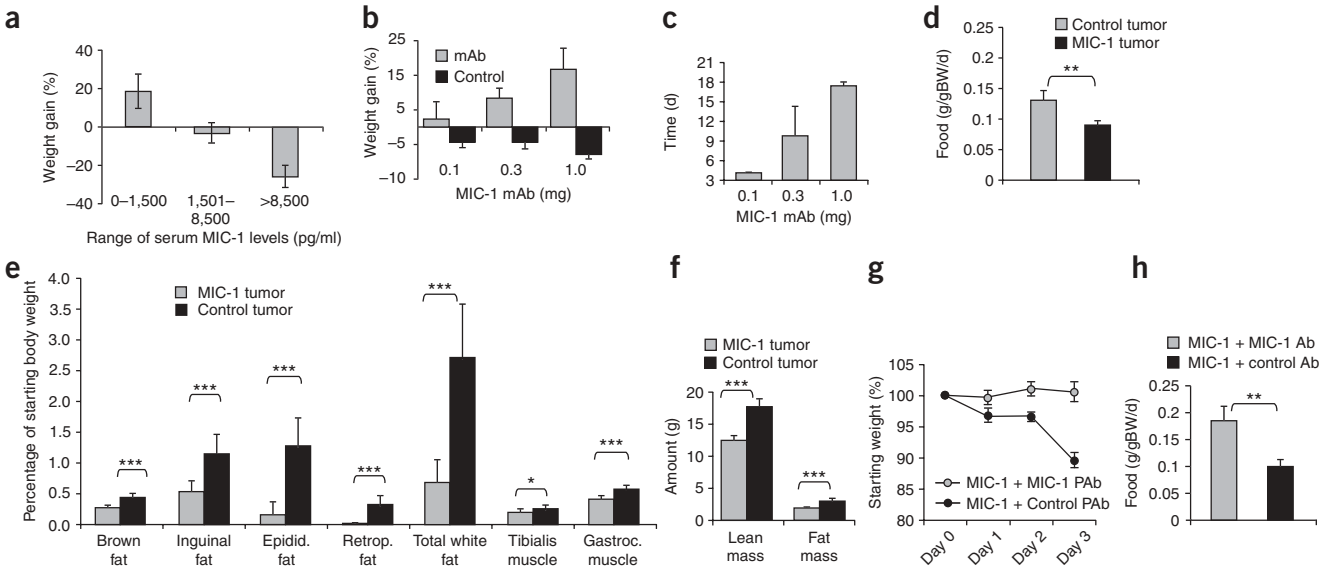

Figure 1 Effect of MIC-1 on mouse weight, food intake and body composition. (**a**) Forty-five nude mice were injected s.c. with DU145 cells expressing human MIC-1 or empty plasmid vector and monitored for 6 weeks. The mean and s.d. of weight change were plotted against serum human MIC-1 levels. (**b**) Nude mice were xenografted with DU145 cells expressing MIC-1. After 11 d, three mice per dose were given a single i.p injection of MIC-1 mAb, and five mice were injected with control buffer (vehicle) or left untreated. The mean and s.d. of their peak weight gains over 20 days are compared to the mean weight change in these control buffer–treated and untreated mice. (**c**) The mean and s.d. of the duration of the response (time to return to what their weight was on the day of antibody injection) of the mice in **b** is plotted against the dose of MIC-mAb. (**d**) Twenty nude mice were xenografted as in **b**. On day 8, when the average weight loss in the MIC-1 mice was 7%, food intake was measured for three consecutive 24-h time periods and the results expressed as the mean and s.d. (**e**) Twenty nude mice were engrafted as in **b**. They were killed when those with MIC-1 tumors had lost approximately 18% body weight. Selected fat and muscle compartments were dissected, removed and weighed. Total white fat represents the summed weight of inguinal, epididymal and retroperitoneal fat depots. The results are the mean and s.d. of the specimen weight as a percent of the weight of the mouse at the day of tumor injection. (**f**) Mice in **e** underwent DXA scanning and the results are expressed as mean and s.d. of total lean and fat mass in grams. (**g**) Twelve BALB/c mice were treated twice daily s.c. with 10 μg of human MIC-1. At the start of the experiment, 50% were given a single i.p. dose of 10 mg of MIC-pAb or CON-pAb. Mice were monitored daily and their weight is expressed as a mean and s.d. percentage of their starting weight. (**h**) The mean and s.d. of daily food intake of the mice in **g** was monitored for three consecutive 24-h time periods. *$P < 0.05$, **$P < 0.01$, ***$P < 0.001$.

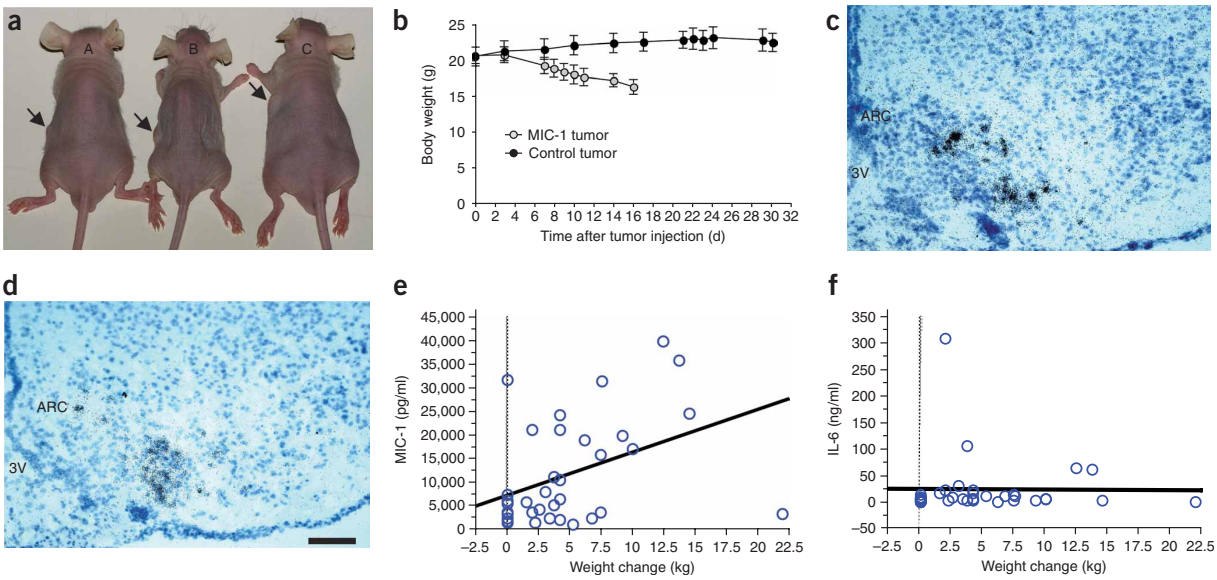

Figure 2 Effect of MIC-1 on body weight in mice and in humans with advanced prostate cancer. (**a**) Representative photograph of a nude mouse xenografted with DU145 cells transfected with empty vector (A), DU145 cells overexpressing MIC-1–14 d post xenografting (B) or a mouse treated like mouse B but given 1 mg MIC-mAb i.p. 9 d earlier (C). Arrow designates site of tumor growth. (**b**) Mean and s.d. of body weight of 40 nude mice xenografted with MIC-1 overexpressing or control tumors. (**c**,**d**) Emulsion autoradiographs of *in situ* hybridization for growth hormone–releasing hormone mRNA in the ARC of a control tumor mouse (**c**) and a MIC-1 expressing tumor mouse (**d**). Analysis of silver grain density over individual neurons indicates a reduction from 100 ± 8% of control to 71 ± 9% of control ($P = 0.0343$) in the MIC-1 tumor mice. ARC, arcuate hypothalamic nuclei; 3V, third ventricle. Scale bar, 40 μm. (**e**,**f**) Correlation between weight change and serum levels of MIC-1 (**e**, $P = 0.0087$; $r = 0.419$) or IL-6 (**f**, $P = 0.9292$; $r = 0.02$) in individuals with advanced prostate cancer.

To directly show the dependence of weight loss on MIC-1, we injected tumor-bearing mice with antibody to MIC-1. A single injection of a monoclonal antibody to human MIC-1 (MIC-mAb) rapidly reversed the weight loss (Figs. 1b,c and 2a and supplementary fig. 1 online) without having any effect on tumor size. Injecting tumor-bearing mice with polyclonal sheep antibody to MIC-1 (MICpAb) similarly reversed weight loss (data not shown). The magnitude and duration of the reversal of MIC-1–induced weight loss was proportional to the amount of MIC-mAb administered. Injection of 1 mg of MIC-mAb led to a peak weight gain of 14%, completely reversing tumor-induced weight loss, with a duration of 17 d (Fig. 1c, supplementary Fig.1) Furthermore, twice daily s.c. administration of increasing doses of human MIC-1 to normal BALB/c mice resulted in a dose-dependent weight loss (supplementary Fig 2. online). Treatment with human MIC-1 (20 μg/day) resulted in marked weight loss that could also be reversed by MIC-pAb but not control sheep IgG (CON-pAb) (Fig. 1g). These data indicate that the weight loss induced by MIC-1–expressing tumors is specifically mediated by MIC-1.

MIC-1–induced weight loss is due to reduced food intake

To more specifically characterize the nature of the weight loss induced by MIC-1–expressing tumors, we determined the changes in fat and lean-tissue mass (Fig. 1e). Mice bearing tumors overexpressing MIC-1 had no remaining retroperitoneal fat and 54% and 89% reductions in inguinal and epididymal fat depots, respectively. There were considerable reductions in the weight of the interscapular brown adipose tissue depot (40%) as well as the tibialis and gastrocnemius muscles (25% and 29%, respectively) (Fig. 1e). Dual-energy X-ray absorptiometry (DXA) scanning data confirmed that mice with MIC-1 tumors lost an average of 5.3 g of lean mass and 1.1 g of fat mass compared to control mice (Fig. 1f).

Mice with DU145-cell tumors overexpressing MIC-1, that were associated with high serum MIC-1 ate, on average, 32% less food than control mice (Fig. 1d). Similarly, administration of recombinant MIC-1 to BALB/c mice resulted in a marked decrease in food intake (Fig. 1h). This hypophagia was reversed by MIC-pAb treatment, which led to weight gain (Fig. 1h). MIC-1 also induced hypophagia and weight loss in massively obese leptin-deficient *ob/ob* mice that were injected twice daily with 10 μg of MIC-1 per 20 g of body weight for 3 d (supplemtary Fig. 3a,b online).

Vehicle-injected BALB/c mice that were fed the same amount as that consumed by

MIC-1 injected mice (pair-fed controls), lost slightly more weight than MIC-1–injected mice. Both groups lost weight compared to *ad libitum*–fed mice (supplementary Fig 4. A,b online). Additionally, when injected with MIC-1, BALB/c mice actually showed a small, but significant, reduction in energy expenditure, as determined by indirect calorimetry (supplementary Fig 5. online). These data establish decreased energy intake as the sole cause of MIC-1–induced weight loss.

This reduction in energy intake by MIC-1 tumor–bearing mice led to substantial reductions in serum concentrations of free fatty acids, triglycerides, glucose, glucagon, leptin and insulin-like growth factor-1 (IGF-1; supplementary Table 1. online), which is consistent with the loss of lean and fat mass by these mice. Changes in circulating IGF-1 abundance suggested that the hypothalamopituitary somatotropic axis was inhibited, which was confirmed by the reduction in growth hormone–releasing hormone mRNA expression in the brains of mice with MIC-1 tumors (Fig. 2c,d). Although lowered serum IGF-1 levels may contribute to some of the effects of MIC-1, notably the loss of lean tissues[15], this change cannot account for the fat loss observed in MIC-1–treated mice, because congenic mice with low serum IGF-1 levels have significantly elevated body fat[16].

MIC-1 tumor–bearing mice also showed a substantial reduction in serum leptin abundance, despite having concurrent hypophagia (supplementary Table 1,). This suggests that MIC-1 overrides the orexigenic effects of lowered serum leptin levels and is consistent with our observation that leptin-deficient *ob/ob* mice also show hypophagia and weight loss in response to MIC-1.

Prostate cancer weight loss correlates with serum MIC-1 level

To determine the relevance of MIC-1 with regard to anorexia and weight loss in humans, we measured serum MIC-1 levels in a previously characterized cohort of individuals with advanced prostate cancer, in whom high serum IL-6 had been associated with cachexia[17]. Among patients with advanced cancer, serum MIC-1 was significantly higher in individuals with cachexia than in those without cachexia (12,416 ± 10,235 pg/ml versus 3,265 ± 6,370 pg/ml (mean ± s.d.); $P < 0.0001$; Mann-Whitney *U*-test), as was serum IL-6 (33.8 ± 64.2 pg/ml versus 7.8 ± 3.4 pg/ml, $P < 0.002$; Mann-Whitney *U*-test). Serum MIC-1 was weakly, but significantly, positively correlated with serum IL-6 levels ($r = 0.2949$, $P < 0.04$; linear regression). In addition, as indicated by single and multivariate logistic regression, both serum MIC-1 and serum interleukin-6 (IL-6) abundances were independent predictors of the presence of cancer-induced cachexia (univariate logistic regression: $P = 0.0002$ and $P < 0.0001$, respectively; multivariate logistic regression, $P = 0.0017$ and $P = 0.0005$, respectively). However, the best objective and quantifiable measure of anorexia and cachexia is weight loss. Serum MIC-1 abundance was significantly associated with the degree of prostate cancer–associated weight loss (Fig. 2e; $P = 0.0087$, $r = 0.419$, linear regression), whereas serum IL-6 showed no such relationship (Fig. 2f; $P = 0.9292$; linear regression).

To assess the possibility that serum MIC-1 estimation may be a useful predictor of prostate cancer–associated anorexia and weight loss, we compared, by receiver operator curve analysis, the serum marker currently used (IL-6) with serum MIC-1 measured at cancer diagnosis. Serum MIC-1 abundance significantly outperformed IL-6 as a predictor of cancer-associated weight loss (area under the curve (AUC) of 0.6829 for MIC-1 versus 0.3505 for IL-6; $P = 0.0046$). To put this value into context, the receiver operator curve analysis of the most widely used serum marker for the diagnosis of prostate cancer, prostate-specific antigen, has an AUC of 0.678 (95% confidence interval, 0.666–0.689)[18]. Consequently, serum MIC-1 measurement may prove useful for the prediction of anorexia and weight loss associated with prostate cancer and may also identify those individuals who might benefit from any future therapy designed to reduce serum MIC-1 abundance.

Serum MIC-1 level is correlated with BMI in chronic renal failure

Chronic renal failure, like advanced cancer, is associated with anorexia, weight loss and cachexia. Weight loss and a lowered body mass index (BMI) are also strong predictors of mortality in end-stage renal failure[19]. We examined the relationship between BMI and serum MIC-1 level in a cohort of 381 individuals with end-stage renal failure[20]. We found that individuals who died during the study period (up to 3 years) had a significantly lower BMI (26.17 ± 5.63; 266 (mean ± s.d.; *n*), 23.15 ± 4.92; 104: $P < 0.0001$; unpaired *t*-test). Serum MIC-1 levels determined in pre-dialysis samples obtained at study entry were significantly and inversely correlated with BMI, such that increasing serum MIC-1 levels were associated with lower BMI ($P = 0.0003$; $r = 0.189$; linear regression). This suggests that in chronic renal failure, as in cancer, elevated MIC-1 may contribute to weight loss.

Transgenic mice overexpressing MIC-1 are smaller and eat less

To estimate the effects of long-term elevated MIC-1, we examined C57/BL6 transgenic mice that overexpressed MIC-1 under the control of the macrophage-specific colony-stimulating factor-1 receptor promoter (fmsMIC-1 mice) (supplementary Fig. 6 online). Although similar in weight to wild-type controls in the first 48 h after birth (Fig. 3a), by 21 days of age, both male and female fmsMIC-1 mice weighed 18% less than sex-matched wild-type littermates (Fig. 3a) and ate less in absolute terms (Fig. 3b). Like mice acutely treated with MIC-1, male and female fmsMIC-1 mice had lower amounts of fat in all measured depots (Fig. 3c,d). Overall, the data from the transgenic mice overexpressing MIC-1 is broadly consistent with mice acutely treated with this cytokine.

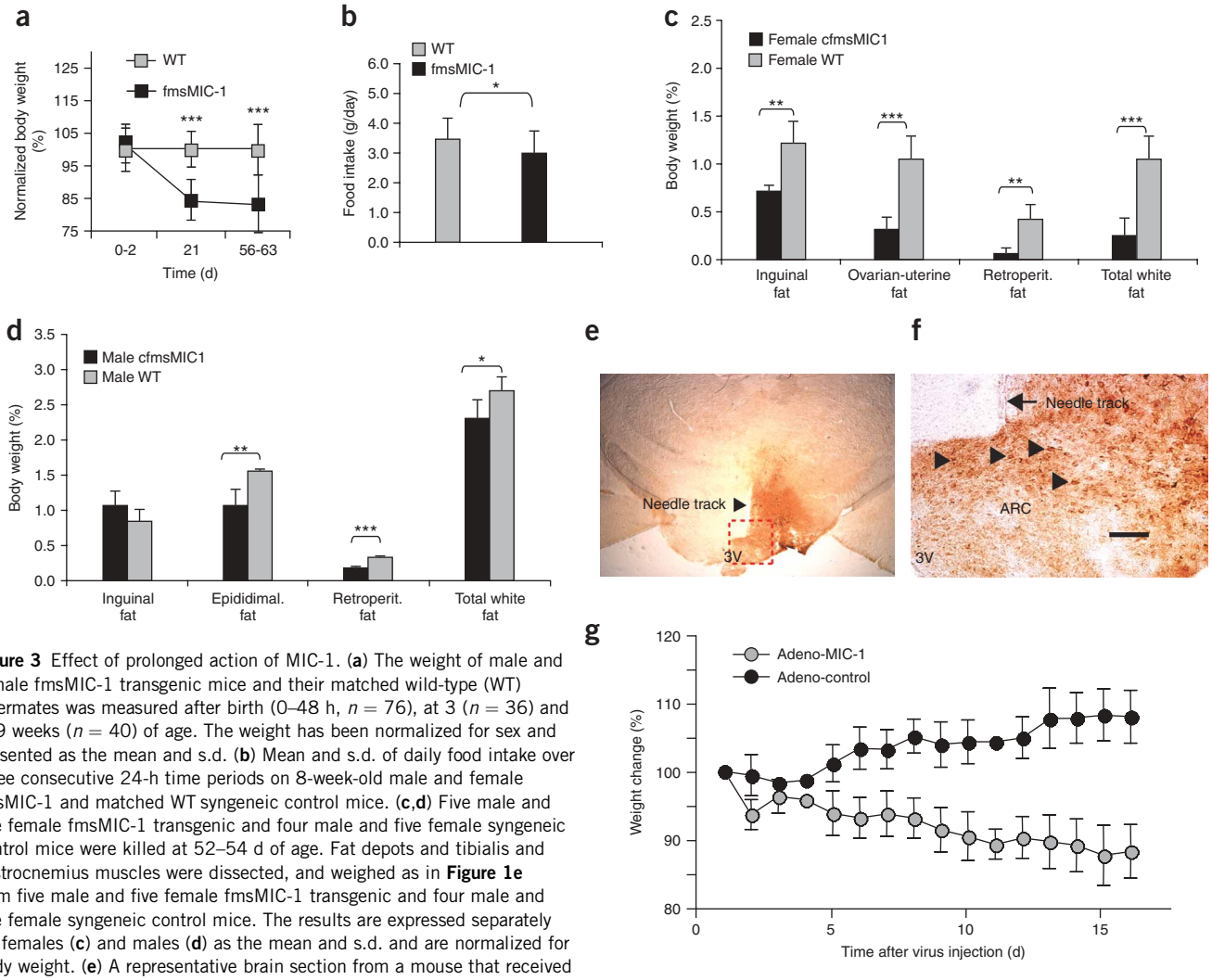

Figure 3 Effect of prolonged action of MIC-1. (**a**) The weight of male and female fmsMIC-1 transgenic mice and their matched wild-type (WT) littermates was measured after birth (0–48 h, $n = 76$), at 3 ($n = 36$) and 8–9 weeks ($n = 40$) of age. The weight has been normalized for sex and presented as the mean and s.d. (**b**) Mean and s.d. of daily food intake over three consecutive 24-h time periods on 8-week-old male and female fmsMIC-1 and matched WT syngeneic control mice. (**c**,**d**) Five male and five female fmsMIC-1 transgenic and four male and five female syngeneic control mice were killed at 52–54 d of age. Fat depots and tibialis and gastrocnemius muscles were dissected, and weighed as in **Figure 1e** from five male and five female fmsMIC-1 transgenic and four male and five female syngeneic control mice. The results are expressed separately for females (**c**) and males (**d**) as the mean and s.d. and are normalized for body weight. (**e**) A representative brain section from a mouse that received a unilateral injection of AAV overexpressing human MIC-1, which is stained with MIC-1 mAb. (**f**) A higher magnification of AAV–MIC-1–expressing hypothalamus shows the neuronal specificity of MIC-1 expression, examples of which are denoted by arrowheads. Scale bar, 40 μm. (**g**) Weight was monitored in 12 mice, half of which received a unilateral hypothalamic injection of AAV–MIC-1 and the other half control AAV vector. Mice were weighed daily and the results are plotted as mean ± s.e.m. *$P < 0.05$, **$P < 0.01$, ***$P < 0.001$.

Systemically administered MIC-1 activates hypothalamic neurons

The major regulatory centers for appetite and weight control are in the hypothalamus, parts of which have a semipermeable blood-brain barrier, potentially allowing for direct interaction with blood-borne mediators[21]. To determine whether MIC-1 might exert its effect directly on the brain, we injected mice intraperitoneally (i.p.) with human MIC-1 and examined the brain expression pattern of the immediate-early oncogene c-fos[22]. There was significantly increased c-fos immunoreactivity in the arcuate (ARC; $P = 0.0036$) and paraventricular nuclei (PVN; $P = 0.001$), implicating the neurons in these nuclei as

downstream mediators of MIC-1 action (supplementary Fig. 7a-d online). The area postrema (AP) (supplementary Fig 7e,f) also showed a significant increase in the number of c-fos–positive neurons (P = 0.0014), suggesting a potential role for this brainstem nucleus in the response to MIC-1.

These findings suggest that the central effect of MIC-1 is directed at the ARC, the major center for appetite control. Projections from the ARC reach other hypothalamic nuclei such as the paraventricular nuclei from which connections are formed with brain stem areas including the area postrema, by which they specifically modulate vagal sympathetic nervous system activity[23]. However, direct MIC-1 activation of the area postrema cannot be excluded. The lack of any change in c-fos activation in the nucleus tractus solitaris (NTS) (data not shown) suggests that afferent signals originating from the periphery via the vagus nerve are not involved in mediating MIC-1 effects.

Hypothalamic overexpression of MIC-1 induces weight loss

To further demonstrate that MIC-1 mediates weight loss via hypothalamic effects, we induced MIC-1 overexpression by direct unilateral injection of adeno-associated virus (AAV) carrying the MIC-1 gene, into the ARC. Immunohistochemistry in these mice demonstrates expression of human MIC-1 by cells in the ARC (Fig. 3e,f), and it is notable that these mice rapidly lost weight (Fig. 3g). Marked MIC-1–induced weight loss (21%) was accompanied by a decrease in food ingestion to 83% that of mice injected with empty AAV (P = 0.04).

Systemic MIC-1 acts on the ARC through the TGF-β RII

TGF-β superfamily proteins, such as MIC-1, bind to and act through a highly conserved receptor superfamily consisting of four distinct type II (RII) and seven distinct type I receptors (RI). Upon ligand binding, the RII transphosphorylates serine residues in the cytoplasmic domain of RI. This triggers a signaling cascade that involves both Smad and non-Smad regulatory pathways.

Immunohistochemistry with antibodies to different RII receptors showed that only the TGF-β RII colocalized with c-fos in the hypothalami of mice injected with MIC-1 (Fig. 4a,b). To determine whether TGF-β RII formed part of the MIC-1–binding receptor complex, we used unilateral hypothalamic injection of blocking antibodies to this receptor. Twenty four hours after this hypothalamic injection, we injected these mice i.p. with 10 μg of MIC-1. Thirty minutes later the mice were killed and their brains examined for hypothalamic c-fos expression. As determined by immunohistochemistry, nuclear c-fos expression was inhibited on the side injected with the TGF-β RII antibody but not on the contralateral side (Fig. 4c–e). Notably, injection of blocking antibodies directed at the RII of bone morphogenetic protein (BMP) or at the leptin receptor did not result in inhibition of MIC-1–induced c-fos expression (Fig. 4f–h). Thus, TGF-β RII is likely to form part of the complex through which MIC-1 exerts its effect in the hypothalamus.

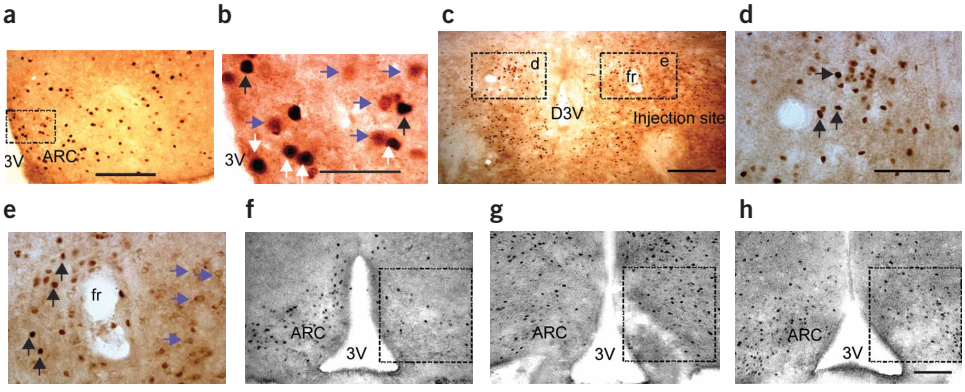

Figure 4 MIC-1 receptor identification. Mice were injected i.p. with 100 μg of MIC-1 and their brains isolated. (**a**) Sections were double labeled with antibodies for TGF-β RII and c-fos (marker of cell activation). Scale bar, 25 μm. (**b**) Higher magnification of the area marked in **a**. Cells are stained with antibody only to TGF-β RII (purple arrowhead), and cell nuclei are stained with antibody to c-fos (black arrowhead). Selected double labeled cells are marked with white arrowheads. Scale bar, 5 μm. (**c**–**e**) Mice were given an intrahypothalamic injection of antibody to TGF-β RII, on the right, as indicated in **c**, followed by an i.p. injection of MIC-1 24 h later. (**c**) Sections were then labeled with a rabbit antibody to c-fos as well as antibody to goat IgG to detect the goat antibody to TGF-β RII that had been directly injected into the hypothalamus. Scale bar, 40 μm (**d**,**e**) High-power views of the areas in **c**. Nuclear c-fos staining is eliminated only on the side of injection of the antibody to TGF-β RII (**e**), but staining of TGF-β RII is clearly visible (purple arrow). Both on the side of intrahypothalamic injection of TGF-β RII antibody but distant from the injection site, and on the contralateral side, is c-fos staining (black arrow). Scale bar, 25 μm. (**f**,**g**,**h**) Unilateral ARC injection of antibody to TGF-β RII (**f**), but not antibody to the leptin receptor (**g**) or BMP RII (**h**), blocks MIC-1–induced c-fos staining. With antibody to TGF-β RII (**f**), this inhibition is confined to the side of injection (right). Scale bar, 40 μm. D3V, dorsal third ventricle; fr, frasciculus retroflexus.

To probe the mechanisms by which MIC-1 induces its downstream effects, we used immunohistochemistry to examine the hypothalamus of mice injected i.p. with 10 μg of MIC-1, and when we did not see a response, we increased the dose to 100 μg. Using antibodies specific for the phosphorylated forms of Smad-2, Smad-3 and Smads 1, 5 and 8, we could not detect any substantial increase in phospho-Smad staining in the MIC-1–treated mice, suggesting that these pathways are not used or that the constitutive activation of these pathways masks any significant increase in Smad phosphorylation. However, MIC-1, but not control buffer, induced phosphorylation of extracellular signal–regulated kinase 1/2 in the ARC (supplementary Fig. 8a-c online), suggesting that MIC-1 may mediate some of its effects via this pathway.

MIC-1 modulates ARC NPY, POMC mRNA and Stat3

As measured by *in situ* hybridization, MIC-1 injection reduced the level of neuropeptide Y mRNA expression in the ARC by 34% and increased pro-opiomelanocortin (POMC) mRNA levels by 47%, consistent with a reduced feeding drive (Fig. 5). This upregulation of the POMC anorexigenic and downregulation of neuropeptide Y orexigenic pathways is similar to the pattern observed in leptin-treated mice. Because of this similarity, we also probed the hypothalamus with antibodies to phosphorylated signal transducer and activator of transcription-3 (P-Stat3), a central molecule activated via the leptin receptor signaling pathway (Fig. 6). We found that MIC-1–induced upregulation of P-Stat3 in neurons in the lateral ARC and ventromedial hypothalamus (Fig. 6b). Notably, the pattern of P-Stat3 staining in MIC-1–treated mice was different from that induced by leptin injection, with the majority of P-Stat3–positive neurons being present in the lateral ARC compared to the dorsal ARC with leptin injection (Fig. 6a). Thus, MIC-1 and leptin induce P-Stat3 in different subsets of ARC neurons, suggesting that they induce their effects through distinct pathways. Indeed, injection of MIC-1 into leptin receptor–deficient *db/db* mice produced P-Stat3 staining in the ARC comparable to that seen in wild-type MIC-1–injected mice (Fig. 6d), showing that MIC-1 does not act through the leptin receptor.

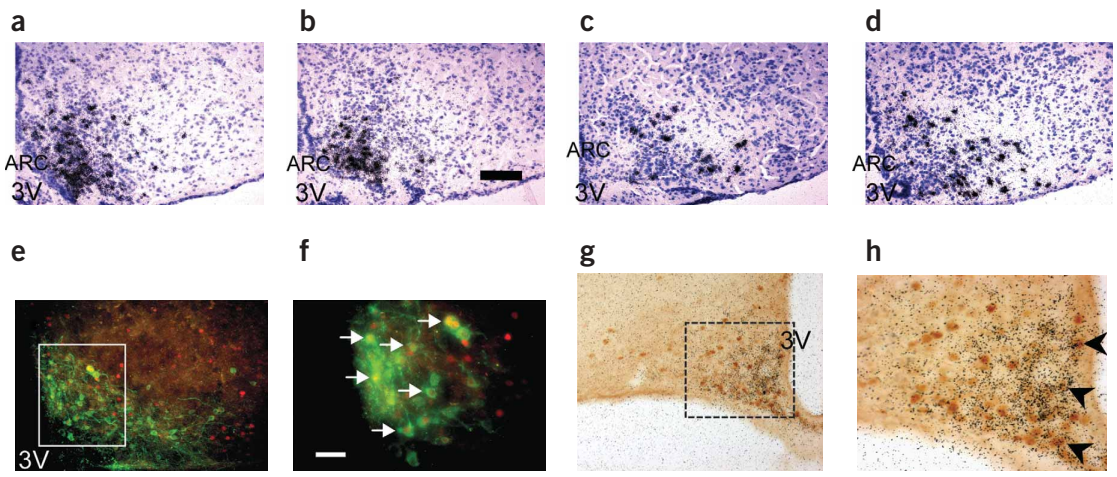

Figure 5 MIC-1 induces alteration in expression of neuropeptide Y and POMC in neurons expressing phosphorylated Stat3. (**a**–**d**) BALB/c mice were injected i.p. with either control buffer (**a**,**c**) or 10 μg human MIC-1 (**b**,**d**). *In situ* hybridization was performed on brain sections isolated 1 h after injection to measure expression of neuropeptide Y (**a**,**b**) and POMC mRNA (**c**,**d**). Expression levels quantified in the ARC relative to control-injected mice indicated a significant downregulation of neuropeptide Y mRNA from 100 ± 13.3% to 66 ± 6.1% of control ($P = 0.0272$) and an upregulation of POMC mRNA from 100 ± 7.6% to 147 ± 10.5% of control ($P = 0.0061$). Scale bar, 40 μm. (**a**-**e**,**g**). Different wild-type BALB/c mice were injected i.p. with 100 μg of human MIC-1, and 30 min after injection the mice were killed and brain sections stained with antibody to P-Stat3 together with immunofluorescent antibody to α-MSH (**e**) to demonstrate colocalization of P-Stat3 (red) and α-MSH (green) within individual cells (arrows in **f**). Boxed area in **e** is enlarged in **f**. *In situ* hybridization for NPYY mRNA combined with immunohistochemistry for P-Stat-3 shows their colocalization (arrowheads) (**g**,**h**). Boxed area in **g** is enlarged in **h.** Scale bar (**f**,**h**), 25 μm.

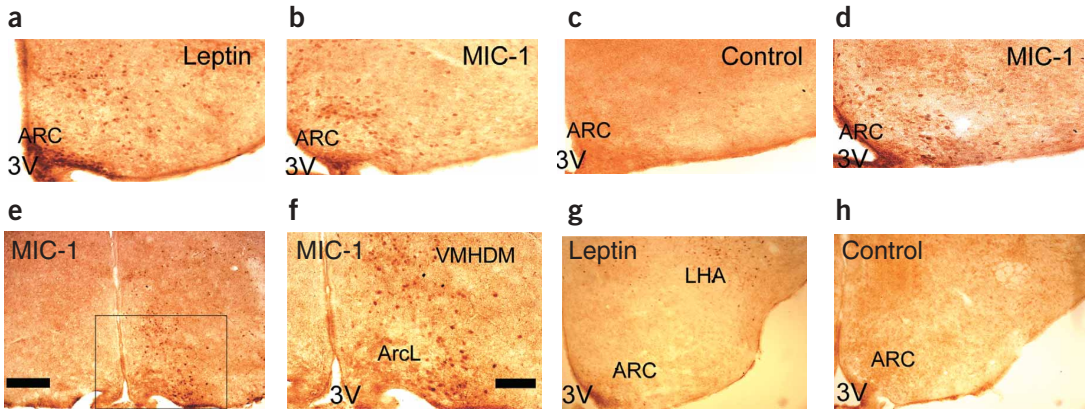

Figure 6 MIC-1, injected systemically or locally, induces Stat3 phosphorylation in the hypothalamus, even in *db/db* mice. (**a**–**d**) Wild-type BALB/c (**a**–**c**) or leptin receptor–deficient *db/db* (**d**) mice were injected i.p. with either 100 μg leptin (**a**), 100 μg human MIC-1 (**b**,**d**) or control buffer (**c**). (**e**–**h**) Wild-type BALB/c mice also received direct unilateral injection into the hypothalamus of either 1 μg of human MIC-1 (**e**,**f**), leptin (**g**) or control buffer (**h**). Either 20 (**e**–**h**) or 30 min (**a**–**d**) after injection, mice were perfused, and their brain sections were stained with antibody to P-Stat3. Scale bars: **a**–**d**,**f**–**h**, 40 μm; **e**, 100 μm.

To identify the MIC-1–induced, P-Stat3–positive neurons, we carried out *in situ* hybridization for *NPY* (the gene encoding neuropeptide Y, Fig. 5g,h) or immunohistochemistry for α-melanocyte–stimulating hormone (α-MSH) (Fig. 5e,f), a biologically active processed product of POMC, along with immunohistochemistry and immunofluorescence for P-Stat3 (Fig. 5e–h). This demonstrates that MIC-1–induced P-Stat3–positive neurons colocalize with α-MSH–staining (Fig. 5e,f) and *NPY*– (Fig. 5g,h) expressing neurons. This identifies neuropeptide Y and POMC neurons as the major class of targets for MIC-1, and it suggests that the reduced food intake leading to weight loss results from altered neuropeptide Y and α-MSH production. Consistently with the c-fos data (supplementary Fig. 7b) the majority of these P-Stat3/neuropeptide Y– and P-Stat3/α-MSH–positive neurons represent a different subset from the ones activated by leptin, suggesting a potential new pathway through which MIC-1 could regulate appetite.

Direct injection of MIC-1 into ARC also activates Stat3

To further demonstrate that MIC-1 acts directly on the ARC, we performed direct unilateral injection of MIC-1, leptin or control buffer into the ARC (Fig. 6e–h). Both MIC-1 (Fig. 6e,f) and leptin (Fig. 6g) clearly induced activation of P-Stat3 in the ARC at 20 min after injection in a pattern similar to that seen with systemic administration. MIC-1 injection induced the phosphorylation of Stat3 in neurons in the lateral ARC and the dorsal ventromedial hypothalamic nucleus (VMHDM) (Fig. 6e,f). In contrast, leptin injection activated the Stat3 pathway in neurons of the dorsal ARC, the dorsal VMHDM and lateral hypothalamic area (Fig. 6g). This supports our contention that these two mediators act on different hypothalamus neuronal subsets.

DISCUSSION

Tumor overproduction of MIC-1 and the correlation of serum MIC-1 levels with weight loss (in both animal models and in individuals with prostate cancer) suggest that MIC-1 is involved in the pathogenesis of cancer anorexia and weight loss and is perhaps involved in other cachectic conditions, such as those that are associated with renal and cardiac failure. Although many studies describe high cytokine levels in individuals with cancer anorexia and cachexia, we are not aware of any studies that have shown a direct correlation of cytokine abundance with a degree of weight loss such as the one we have shown with MIC-1. This relationship, as well as our finding that MIC-1 acts on TGF-β RII receptors in hypothalamic neurons and thereby may decrease appetite, suggest that MIC-1 is a key inducer of cancer-related anorexia and weight loss. Additionally, the reversal of weight loss caused by treatment with antibodies to MIC-1 raises the possibility that therapeutic antibodies may be used to treat this serious disorder. MIC-1 induces hypophagia and affects the major hypothalamic regulators of food intake and energy homeostasis, neuropeptide Y and POMC-derived α-MSH. Although MIC-1 triggers effects similar to those induced by leptin, such as anorexia, weight loss, a decrease in hypothalamic neuropeptide Y and an increase in POMC expression, there are differences in the subset of neuropeptide

Y and POMC neurons activated by MIC-1. This suggests there is a more diverse functional network of neurons regulating different aspects of energy homeostasis than was previously thought. Taken together, the data in this study show that MIC-1 is a previously unknown central regulator of appetite and weight and is a potential target for the treatment of cancer anorexia and weight loss, as well as of obesity.

METHODS

Ethics committee approval.

All mouse experiments were approved by the Garvan and the St. Vincent's Hospital Animal Ethics Committees. The human studies described were done with informed consent from study subjects and with the approval of either the Institutional Review Board of the University of Washington or the Hennepin County Medical Center/Minneapolis Medical Research Foundation/Hennepin Faculty Associates Human Subject Research Committee.

Tumor xenograft model.

We injected 8-week-old BALB/c nude mice s.c. on their right flanks with 5 X 10^6 to 7 X 10^6 transfected DU145 cells in 200 ml of PBS. The DU145 cells had been transfected with either the pIRES2-EGFP plasmid (Clontech) containing either mature MIC-1 (MIC-1), full length MIC-1, a proconvertase site-deletion mutant of MIC-1 or empty vector[11]. Once tumors were visible, we measured tumor size and weighed the mice every 1–3 days for 6 weeks.

We determined lean and fat mass both by DXA (Lunar Piximus II, GE Medical Systems) and by dissection of white and brown adipose tissue depots and tibialis and gastrocnemius muscles. We then expressed these weights as a proportion of the body weight of the mouse on the day of the tumor injection.

We measured food consumption by placing food into the hopper, which was weighed at time 0, and then we determined the amount of food consumed at 24 h intervals by subtracting refusal and spillage from the food put into the hopper.

Arcuate hypothalamic nucleus injection of AVV–MIC-1.

Adult male mice were anesthetized i.p. with a single dose of ketamine and xylazine (100 mg/kg and 20 mg/kg, respectively) and placed on a Kopf stereotaxic frame (David Kopf Instruments). We injected 1 μl AAV–MIC-1 or control 'empty' AAV unilaterally into the ARC at a rate of 0.1 μl/min with a 10-μl Hamilton syringe attached to a Micro4 Micro Syringe Pump Controller (World Precision Instruments, Inc.). We injected for 10 min and then left the needle in place for a further 15 min to allow for diffusion away from the needle tip. The injection coordinates were as follows (distance from bregma): anterioposterior, -1.94 mm; mediolateral, -0.3 mm; dorsoventral, -5.8 mm; this corresponded to the ARC hypothalamic nucleus[24, 25]. We always performed the injections between 10 a.m. and 12 p.m.

Mouse intrahypothalamic injection.

We anesthetized the mice, placed them in a Kopf stereotaxic frame and injected them unilaterally with a Hamilton syringe as indicated above.

For direct injection of cytokines, we injected adult wild-type mice with 1 μl MIC-1, 1 μl leptin or 1 μl control solution using the following coordinates (distance from bregma): posterior, -1.94 mm; lateral, -0.3 mm; ventral, -5.8 mm; this corresponded to the ARC[25]. Thirty minutes after the start of injection, we killed the mice. We fixed the brains by perfusion and P-Stat3 neurons were identified by immunohistochemistry as indicated below.

For experiments involving the injection of TGF-β receptor antibodies, we injected 1.5 μl of antibody (0.1 mg/ml) unilaterally into the posterior hypothalamic areas of three adult mice at a rate of 0.1 μl/min. The injected antibody was inhibitory goat antibody to TGF-β RII (R&D Systems), BMP RII (GeneTex, Inc.) or leptin receptor (Upstate). The needle was left in place for 10 min after injection to allow diffusion away from the injection site. The injection coordinates were as follows (distance from bregma): anterioposterior, -2.3 mm; mediolateral, -0.5 mm; dorsoventral, -4.5 mm; this corresponded to the posterior hypothalamic area[25]. Twenty-four hours after TGF-β RII antibody injection, we injected mice i.p. with 100 μg of human MIC-1. Exactly 30 min after injection, we killed the mice and collected the brains for detection of c-fos and TGF-β RII immunoreactive neurons in the posterior hypothalamic area as described below.

In an alternative experiment, we divided six adult male mice into three groups and injected the following antibodies into the ARC: 1.5 μl TGF-β RII antibody (0.1 mg/ml), 1.5 μl BMPRII antibody (0.1 mg/ml) or 1.5 μl leptin antibody (0.1 mg/ml). The needle was left in place for 10 min after injection to allow for diffusion away from the injection site. The injection coordinates were as follows (distance from bregma): anterioposterior, -1.94 mm; mediolateral, -0.3 mm; dorsoventral, -5.8 mm; this corresponded to the ARC hypothalamic nucleus[25]. Twenty-four hours after antibody injection, animals were injected i.p. with 100 μg of human MIC-1; 30 min later, the mice were killed and brains were collected for detection of c-fos immunoreactivity in the ARC hypothalamic area as described in the supplementary methods online.

Additional methods.
Information on the generation of MIC-1-overexpressing transgenic mice, MIC-1 reagents and production of AAV vector engineered to express MIC-1, the determination of metabolic rate, respiratory exchange ratio, and physical activity, as well as details about the pair-feeding experiment, the cancer cachexia patient cohort, immunohistochemistry and immunofluorescence of mouse brain, *in situ* hybridization, combined immunohistochemistry and *in situ* hybridization, and statistical analysis are available in the supplementary methods

ACKNOWLEDGMENTS
This work was supported by grants from the National Health and Medical Research Council of Australia (NHMRC), Cancer Council New South Wales, the Richard M. Lucas Foundation and a New South Wales Health Research and Development Infrastructure grant. A.S. and H.H. are both recipients of NHMRC Fellowships and D.A.B. is a Neil Hamilton Fairley Postdoctoral Fellow of the NHMRC. We would like to thank D. Hume (Institute for Molecular Biosciences, The University of Queensland) for the gift of the promoter construct used to create the transgene for the fmsMIC transgenic mice and P. Sawchenko for critical evaluation of this manuscript. This work is dedicated to the memory of Mary Christine Kennedy.

REFERENCES
1. Tisdale, M.J. Cachexia in cancer patients. Nat. Rev. Cancer 2, 862–871 (2002).
2. Huhmann, M.B. & Cunningham, RS. Importance of nutritional screening in treatment of cancer-related weight loss. Lancet Oncol. 6, 334–343 (2005).
3. Marks, D.L., Ling, N. & Cone, RD. Role of the central melanocortin system in cachexia. Cancer Res. 61, 1432–1438 (2001).
4. Rubin, H. Cancer cachexia: its correlations and causes. Proc. Natl. Acad. Sci. USA 100, 5384–5389 (2003).
5. Rall, L.C. & Roubenoff, R. Rheumatoid cachexia: metabolic abnormalities, mechanisms and interventions. Rheumatology (Oxford) 43, 1219–1223 (2004).
6. Anker, S.D. & Sharma, R. The syndrome of cardiac cachexia. Int. J. Cardiol. 85, 51–66 (2002).
7. Bootcov, M.R. et al. MIC-1, a novel macrophage inhibitory cytokine, is a divergent member of the TGF-b superfamily cluster. Proc. Natl. Acad. Sci. USA 94, 11514–11519 (1997).
8. Welsh, J.B. et al. Large-scale delineation of secreted protein biomarkers overexpressed in cancer tissue and serum. Proc. Natl. Acad. Sci. USA 100, 3410–3415 (2003).
9. Buckhaults, P. et al. Secreted and cell surface genes expressed in benign and malignant colorectal tumours. Cancer Res. 61, 6996–7001 (2001).
10. Koopmann, J. et al. Serum macrophage inhibitory cytokine 1 as a marker of pancreatic and other periampullary cancers. Clin. Cancer Res. 10, 2386–2392 (2004).
11. Bauskin, A.R. et al. The propeptide mediates formation of stromal stores of proMIC-1: Role in determining prostate cancer outcome. Cancer Res. 65, 2330– 2336 (2005).
12. Hsiao, E.C. et al. Characterization of growth-differentiation factor 15, a transforming growth factor b superfamily member induced following liver injury. Mol. Cell. Biol. 20, 3742–3751 (2000).

13. Schober, A. et al. Expression of growth differentiation factor-15/ macrophage inhibitory cytokine-1 (GDF-15/MIC-1) in the perinatal, adult, and injured rat brain. J. Comp. Neurol. 439, 32–45 (2001).

14. Bauskin, A.R. et al. Role of MIC-1 in tumorigenesis and diagnosis of cancer. Cancer Res. 66, 4983–4986 (2006).

15. Kamel, H.K., Maas, D. & Duthie, E.H. Role of hormones in the pathogenesis and management of sarcopenia. Drugs Aging 19, 865–877 (2002).

16. Rosen, C.J. et al. Congenic mice with low serum IGF-I have increased body fat, reduced bone mineral density, and an altered osteoblast differentiation program. Bone 35, 1046–1058 (2004).

17. Pfitzenmaier, J. et al. Elevation of cytokine levels in cachectic patients with prostate carcinoma. Cancer 97, 1211–1216 (2003).

18. Thompson, I.M. et al. Operating characteristics of prostate-specific antigen in men with an initial PSA level of 3.0 ng/ml or lower. J. Am. Med. Assoc. 294, 66–70 (2005)

19. . Kovesdy, C.P., Anderson, J.E. & Kalantar-Zadeh, K. Inverse association between lipid levels and mortality in men with chronic kidney disease who are not yet on dialysis: effects of case mix and the malnutrition-inflammation-cachexia syndrome. J. Am. Soc. Nephrol. 18, 304–311 (2007).

20. Apple, F.S., Murakami, M.M., Pearce, L.A. & Herzog, C.A. Predictive value of cardiac troponin I and T for subsequent death in end-stage renal disease. Circulation 106, 2941–2945 (2002).

21. Naylor, J.L. et al. Further evidence that the blood/brain barrier impedes paraquat entry into the brain. Hum. Exp. Toxicol. 14, 587–594 (1995).

22. Karl, T. et al. Y1 receptors regulate aggressive behavior by modulating serotonin pathways. Proc. Natl. Acad. Sci. USA 101, 12742–12747 (2004).

23. Bouret, S.G. et al. Formation of projection pathways from the arcuate nucleus of the hypothalamus to hypothalamic regions implicated in the neural control of feeding behavior in mice. J. Neurosci. 24, 2797–2805 (2004).

24. Lin, E.J. et al. Combined deletion of Y1, Y2, and Y4 receptors prevents hypothalamic neuropeptide Y overexpression–induced hyperinsulinemia despite persistence of hyper-phagia and obesity. Endocrinology 147, 5094–5101 (2006).

25. Paxinos, G. & Franklin, K.B.J. The mouse brain in stereotaxic coordinates (Academic Press, San Diego, USA, 2001).